SCIENTIFIC REPORTS

OPEN

SUBJECT AREAS:
HERPES VIRUS
ANTIVIRAL AGENTS
NANOPARTICLES

Received
12 March 2014

Accepted
11 June 2014

Published
3 July 2014

Correspondence and requests for materials should be addressed to R.T. (rtandon@umc.edu)

Inhibition of cytomegalovirus infection and photothermolysis of infected cells using bioconjugated gold nanoparticles

Bernadette M. DeRussy[1], Madeline A. Aylward[1], Zhen Fan[2], Paresh C. Ray[2] & Ritesh Tandon[1]

[1]Department of Microbiology, University of Mississippi Medical Center, 2500 North State Street, Jackson, MS 39216, USA, [2]Department of Chemistry and Biochemistry, Jackson State University, 1400 J.R Lynch Street, Jackson, MS 39217, USA.

Human cytomegalovirus (CMV) is a herpesvirus that causes major health problems in neonates as well as in immunocompromised individuals[1]. At present, a vaccine is not available for CMV infection and the available antiviral drugs suffer from toxicity, poor efficacy and resistance[1,2]. Here, we chemically conjugated a monoclonal antibody raised against CMV surface glycoprotein (gB) with gold nanoparticles (GNP) and characterized the potential of this gB-GNP conjugate for antiviral activity against CMV. The gB-GNP blocks viral replication, virus-induced cytopathogenic effects and virus spread in cell culture without inducing cytotoxicity. High concentrations of gB-GNP that coat the surface of virus particles block virus entry, whereas lower concentrations block a later stage of virus life cycle. Also, cells treated with gB-GNP gain resistance to CMV infection. In addition, infected cells when bound to gB-GNP can be selectively lysed after exposing them to specific wavelength of laser (nanophotothermolysis). Thus, we have not only designed a potential antiviral strategy that specifically blocks CMV infection at multiple stages of virus life cycle, but we have also characterized a technique that can potentially be useful in eliminating CMV infected cells from donor tissue during transplant or transfusion.

Even in the 21st century, viral infections pose a major threat to both human and animal populations, as designing good antiviral strategies remains challenging. Human cytomegalovirus (CMV) is a herpesvirus, which spreads by contact and is acquired by the majority of the population worldwide by the age of 40 years; however, like most other herpesviruses, it remains in a latent state in healthy individuals without causing any clinical symptoms. Primary CMV infection or reactivation from latency can cause significant health problems in immuno-compromised individuals such as AIDS patients and organ transplant recipients. CMV is also the leading infectious cause of congenital disease in newborns[1]. Despite being designated a pathogen of high priority for the development of a vaccine by the Institute of Medicine, neither a vaccine nor any antiviral agents have been approved yet for treating congenital CMV infection[1]. Moreover, the drugs that are available for use in other clinical settings suffer from safety, efficacy and resistance issues[2]. The current manuscript reports a new bioengineering strategy that combines the specificity afforded by monoclonal antibodies and the multifunctional properties of gold nanoparticles in order to control CMV infection.

Nanobiotechnology-based approaches have shown a great promise for counteracting several pathogens as well as cancers[3–5,11]. Gold nanosystems are particularly attractive because of their unique size-dependent optical properties as well as lack of toxicity in several tested biological systems[6–8]. Gold nanoparticles (GNP) can also serve as "light-directed nano heaters" and this property makes them useful for selective laser photothermolysis[9,10]. GNP derivatives bound to antibodies, aptamers or peptides exhibit high binding affinity and targeted selectivity[4,12,13]. Here, we conjugated a monoclonal antibody raised against human CMV surface glycoprotein (B) with GNP. We synthesized three different types of GNP with different surface properties: spherical (GNPsp)[14], star (GNPst)[15] and popcorn (GNPop)[5,16,17]. All three types of conjugated GNP show inhibitory activity against CMV infection in our experiments.

Covalent immobilization of the monoclonal anti gB antibody onto the surface of the GNP was performed using 4 amino-thio phenol (4-ATP) and a glutaraldehyde spacer method (Fig. 1)[5]. gB-GNP preparations were first tested for their efficacy to block CMV infection of primary human foreskin fibroblasts (HF). Cells were treated with gB-GNP (50 ng/ml conjugated antibody in cell culture medium) for one hour prior to infection with AD169 strain of human CMV at a multiplicity of infection (MOI) of 3.0. This virus has an eGFP marker fused to the C-terminal of the UL32 gene allowing virus replication to be monitored by eGFP fluorescence[18]. At 3 days post

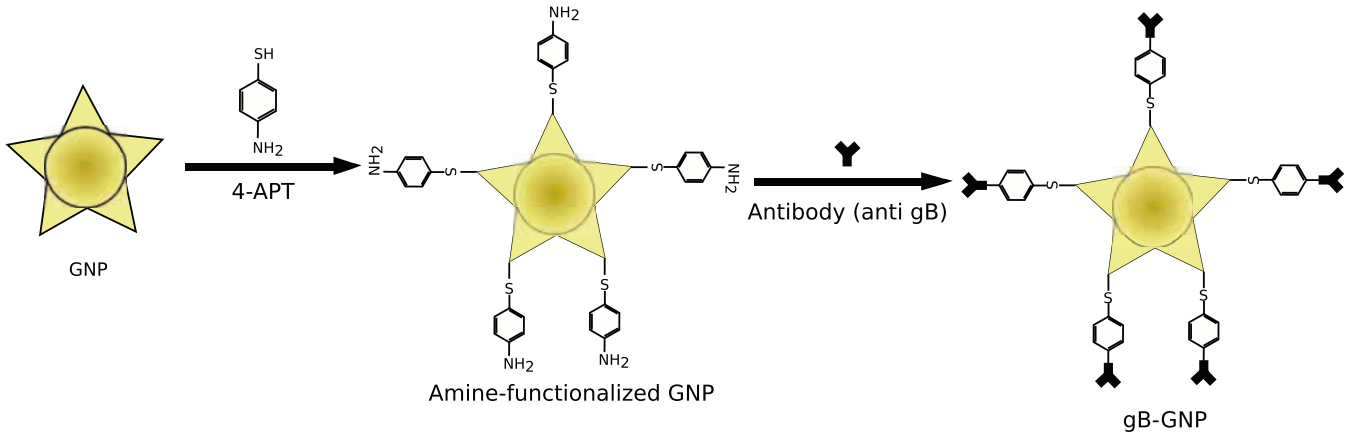

Figure 1 | A schematic representation of the synthetic protocol of monoclonal antibody conjugation with the gold nanoparticles (GNP). We used 4 amino-thio phenol (4-ATP) and a glutaraldehyde spacer method[22] for covalent immobilization of the monoclonal anti gB antibody onto the surface of nanoparticles. Schematic is not drawn to scale.

infection (dpi), presence of virus encoded eGFP fluorescence in untreated cells but not in gB-GNP treated cells indicated that all three types of gB-GNP successfully blocked CMV infection (Fig. 2A–H). The cytopathogenic effects evident in bright-field images in the absence of gB-GNP treatment (Fig. 2A) were not apparent in the treated cells (Fig. 2B–D). Also, when gB-GNPop were added to AD169 infected HF at one dpi, only primary infected cells showed eGFP fluorescence in gB-GNPop treated cells at 3 dpi, whereas both the primary and secondary infected cells showed fluorescence in untreated cells (Fig. 2I–P). This was true for high (1.0) (Fig. 2M, N) as well as low (0.1) (Fig. 2O, P) MOI. Thus, gB-GNPop blocked AD169 spread as well as primary infection in HF. Similar results were obtained for the Towne strain of human CMV as well (extended data 1) however, cytopathogenic effects induced by simian cytomegalovirus (SCMV) infection of HF were not inhibited by gB-GNPop treatment (extended data 2). Also, HSV-1 infection of HF was not abolished due to gB-GNPop treatment (extended data 3), consistent with the specificity of gB-GNPop for CMV gB. The fluorescence in HSV infected cells did reduce slightly upon gB-GNPop treatment suggesting some non-specific interference with HSV particles (extended data 3). One-step growth curve analysis showed significant reduction in CMV (Towne-BAC) titers when treated with gB-GNPop (Fig. 2 Q) and the final viral yields were at least 10,000 fold less than virus yields from untreated cells. We also tested clinical strain of human CMV derived from FIX-BAC that can infect endothelial cell lines[19]. HMEC-1[20] cells infected with FIX virus showed a significant reduction in the expression of viral IE1 protein in gB-GNPop treated cells compared to untreated cells, probed by immunofluorescence at 8 hours post infection (hpi) (extended data 4 A, D). Viral encoded eGFP showed a similar pattern of reduced fluorescence in treated cells (extended data 4 C, F). Thus gB-GNPop successfully blocked entry of a clinical strain of HCMV in these cell types making this approach more clinically relevant. To test whether these conjugated nanoparticles affect cell viability, HF were treated with the working concentration of gB-GNP (50 ng/ml antibody total) (data not shown) as well as double the concentration (100 ng/ml antibody total) at the time of infection and cell viability was recorded at 8 hpi and also at 5 dpi using trypan blue exclusion assay (Fig. 3). All three types of gB-GNP showed little to no toxicity in HF at this time. Only gB-GNPst showed some level of cytotoxicity, which did not develop until 5 dpi (Fig. 3B). The results show that gB-GNP are generally not cytotoxic at the concentration at which they block HCMV infection.

To visualize the binding of gB-GNP to virus particles, purified AD169 virions were incubated with gB-GNP on ice for 30 minutes, then placed on a grid for transmission electron microscopy (TEM) and finally fixed for imaging. Electron micrographs show that higher concentrations of gB-GNP (conjugated to 100 ng antibody total) completely coat the individual virions (Fig. 4A), whereas lower concentrations of gB-GNP (conjugated to 50 ng antibody total) facilitate the aggregation of virions into clusters (Fig. 4B, C).

We then determined the stage of virus replication block mediated by gB-GNP. HF were pretreated with GNPsp, GNPst or GNPop (50 ng/ml conjugated antibody in cell culture medium) for one hour prior to infection with AD169 virus at an MOI of 3.0. Cells were lysed at 6 hpi and probed for viral IE1 protein expression in an immunoblot. At this concentration of gB-GNP, virus entry was intact (Fig. 5A); however at twice the concentration of conjugated antibody (100 ng/ml), virus entry was significantly reduced for gB-GNPsp and GNPop (Fig. 5B and data not shown). This shows that CMV entry in HF is not inhibited at concentrations of gB-GNP that are sufficient to significantly reduce CMV replication (Fig. 2). Thus, impact of gB-GNP on CMV is most likely to be both at the entry and at a later stage of the virus replication.

We utilized the nanophotothermal properties of gB-GNP to test the ability of gB-GNP to induce specific cell lysis of infected cells upon laser exposure. When GNP are exposed to a specific wavelength of laser, they generate heat that selectively kills cells or organisms attached to them[4]. gB-GNPop were added to infected or mock-infected HF at 5 dpi. After binding for 1 hour, excess gB-GNPop were washed off, so that only gB-GNPop that remain attached to infected cells are present on cells. Cells were exposed to light from a 670 nm, 100 mW laser for 15 minutes and then subjected to a cell viability test (MTT). Only cells, which were infected and then treated with gB-GNPop (Fig. 6A) were lysed in this experiment leaving the uninfected or untreated cells viable. GNP conjugated to an unrelated antibody did not result in cell lysis in this experiment (data not shown). These results were also confirmed by testing a range of MOI of HCMV (0.001 to 5.0) on HF. In addition to showing the specificity of gB-GNPop mediated cell lysis upon laser exposure, this experiment showed that increasing the amount of infected cells in the sample leads to increased cell lysis (Fig. 6B). To find out how the temperature increases during nanophotothermolysis, we performed thermal imaging during the exposure using a MikroShot Camera, as we have reported before[4,5,15]. We found that the temperature increased to about 50°C when antibody conjugated nanoparticle-bound purified virus was exposed to the 670 nm laser at 1.5 W/cm^2. Using the same conditions, the temperature increased to only 31°C for the sample containing purified virus and no nanoparticles.

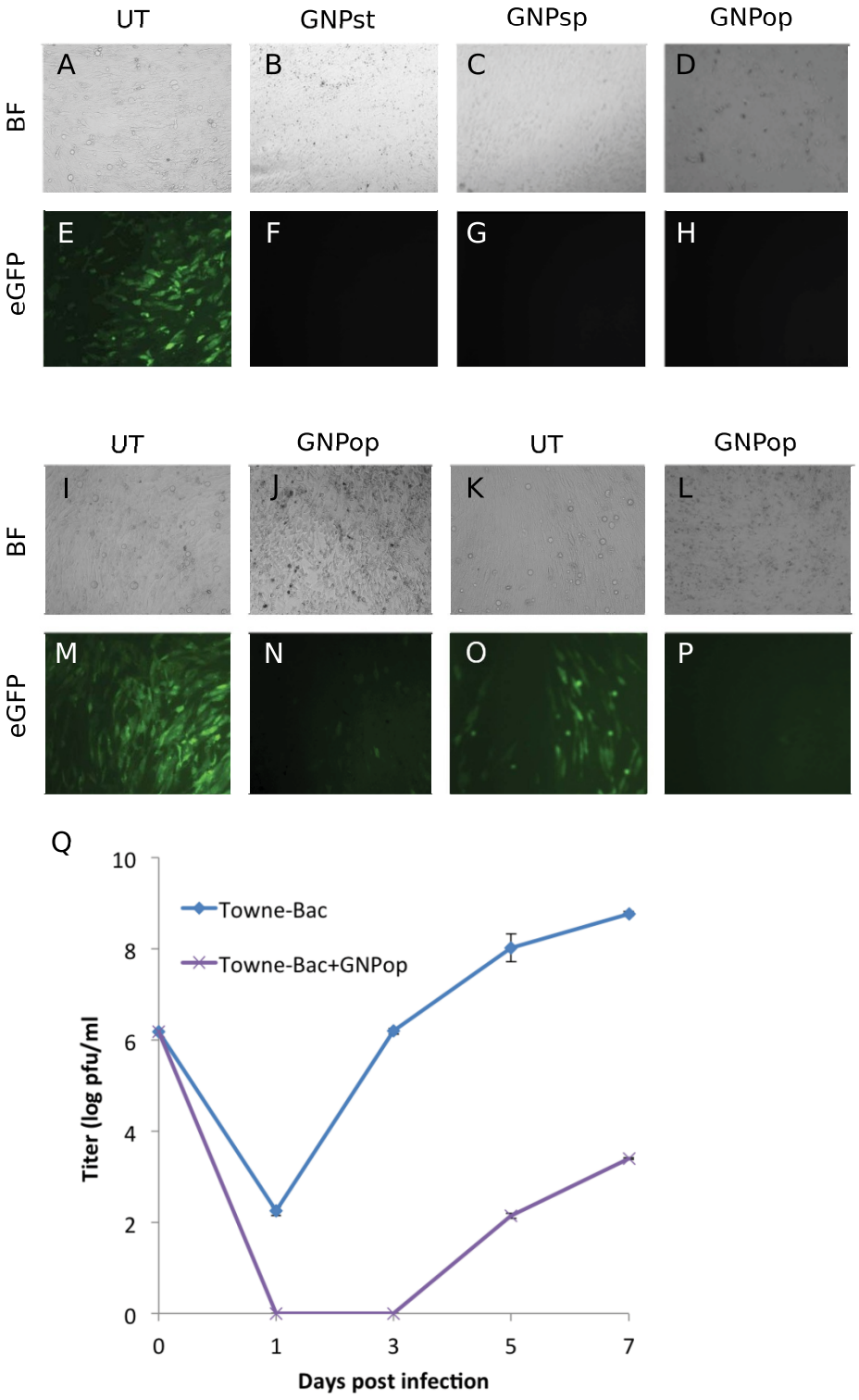

Figure 2 | Effect of anti gB antibody-conjugated nanoparticles on CMV infection of HF cells. (A–H) gB-GNP were tested for their efficacy to block human cytomegalovirus (CMV) infection of primary HF cells. Star (GNPst), sphere (GNPsp) or popcorn (GNPop) shaped nanoparticles were added (50 ng antibody total) to HF at the time of infection, or the cells were mock treated (UT). eGFP fluorescence or bright-field (BF) images were recorded at 5 dpi. eGFP signal emanates from the virus genome. (I–P) gB-GNPop were tested for their efficacy to block the spread of cytomegalovirus infection in HF cells. gB-GNPop (50 ng antibody total) were added to HF at one dpi or the cells were mock treated (UT). eGFP fluorescence or bright-field (BF) images were recorded at 5 dpi. (Q) Single step growth curve analysis of Towne strain of CMV in HF either treated with gB conjugated GNPop (Topwne-Bac + GNPop, 50 ng antibody total) or mock treated (Towne-Bac).

Thus, gB-GNP specifically inhibit HCMV infection as well as virus spread in fibroblast culture without inducing cytotoxicity. Based on TEM, high concentrations of gB-GNPop (conjugated to 100 ng anti gB antibody total) completely coat the virus particles or agglomerate the virus particles in clusters, both interfering with virus entry into cells. Lower concentrations of gB-GNPop (conjugated to 50 ng anti gB antibody total) do not block virus entry but block a later stage of the virus life cycle based on the data from immunofluorescence and

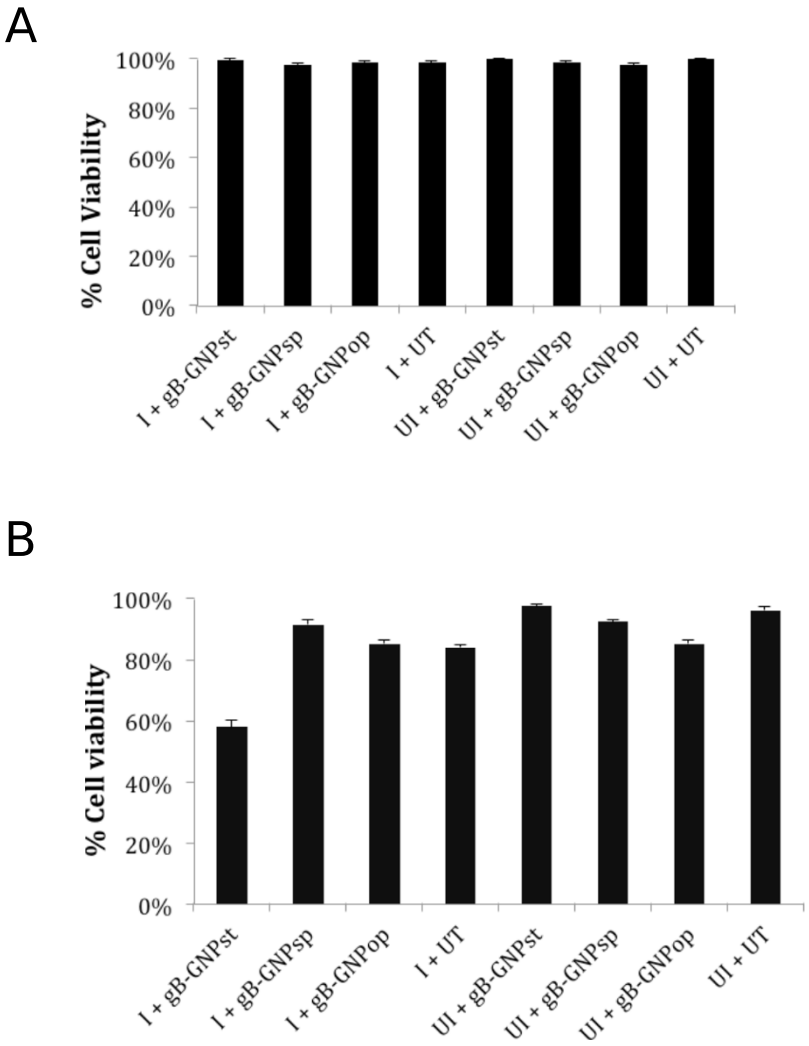

Figure 3 | Viability of HF cells upon gB-GNPsp, gB-GNPst or gB-GNPop treatment. Nanoparticles (conjugated to 100 ng anti gB antibody total) were added to HF at the time of infection (I) with CMV (AD169) at an MOI of 3.0 or the cells were mock-infected (UI) and/or mock-treated (UT). Cell viability was recorded at 8 hpi (A) or at 5 dpi (B) using trypan blue exclusion assay.

growth curve experiments. This stage would most likely to be the virus maturation stage where virus glycoproteins are required for virus envelopment[21]. Although results from SCMV and HSV experiments suggest specificity of gB-GNPop, we did see a slight reduction in HSV (K26GFP) fluorescence in gB-GNPop treated cells suggesting that these particles may non-specifically interfere with virions, likely due to charge-charge interactions. The nanophotothermal properties of gB-GNP can be utilized to selectively kill HCMV infected cells, which will be uniquely useful for preventing HCMV transmission in organ transplants and blood transfusion settings where donor tissue can be treated with gB-GNP and the infected cells can then be eliminated by nanophotothermolysis. gB-GNP can also be engineered to insert an iron core, which will be useful for the magnetic separation of particles along with any attached virus or infected cells from a sample. We are also testing a similar bioconjugated nanoparticle based approach for eliminating infected cells in blood and bone marrow samples. We believe that these antibody-conjugated nanoparticles will become a completely new line of treatment for viral infections and other maladies for which specific biomarkers are known.

Methods

Nanoparticle synthesis and bioconjugation. Gold nanoparticles of 30 nm in size were synthesized by using 0.01 wt.% chlorauric acid and 1 wt.% trisodium citrate dehydrate, as reported earlier[22]. Gold nano-popcorn were synthesized using a two-step process, described earlier[22]. First, small size spherical seed particles were made using hydrogen tetrachloroaurate, trisodium citrate and sodium borohydride. For spherical gold seed synthesis we used 0.025 μM $HAuCl_4 \cdot 3\ H_2O$, 0.01 μM trisodium citrate and 0.01 M sodiumborohydride. Next, we used cetyltrimethylammonium bromide (CTAB) as a shape-templating surfactant to synthesize popcorn-shaped nanoparticles[16]. For this purpose, we added 0.01 g of CTAB in 46.88 mL of H_2O and 0.3 mL of 0.01 M $AgNO_3$ in the seed solutions. For nanostar preparation, we also used a two-step process[23]. First, small size spherical seed particles were synthesized, as for nano-popcorn synthesis. Next, higher concentration of CTAB (0.1 gm CTAB in 46.88 ml H_2O) was used with 0.3 ml 0.01 M AgNO3, which produced gold nano-star. The particle concentration was measured by UV/Vis spectroscopy using the reported molar extinction coefficients at the wavelength of the maximum absorption of each gold colloid[22–24].

Covalent immobilization of the monoclonal anti gB antibody onto the surface of the gold nanoparticles was performed using 4- amino-thio phenol (4-ATP) and a glutaraldehyde spacer method (Fig. 1) as reported earlier[5]. Initially, to avoid non-specific interaction, nanoparticles were coated with thiolated polyethylene glycol (HS- PEG). The nanoparticle surface was then modified by adding amine groups using 4-ATP using our reported method[24]. Briefly, 20 mM 4-ATP was added to 50 mL of gold nanoparticle and the solution was kept at 50°C for several hours under constant sonication. Excess ATP was removed by centrifugation at 8000 rpm for several minutes. 10 mL of amine-functionalized nanoparticles were dispersed into 0.01 M PBS (pH 7.4) containing 5% glutaraldehyde for about 1 hour[24]. These particles were then collected by centrifugation, dispersed in PBS, and incubated with the antibody for 12 h at 4°C. The antibody-modified gold nanoparticles were washed with PBS to remove excess antibody and kept at 4°C in pH 7.4 PBS. To measure the number of antibody molecules binding to each type of gold nanoparticle, we utilized a dye-labeled antibody (goat anti mouse IgG (H + L) secondary antibody DyLight-594 conjugate, Thermo Scientific, Rockford, Il). We dissolved the gB antibody-conjugated gold nanoparticles in potassium cyanide to oxidize the gold nanoparticles, as reported

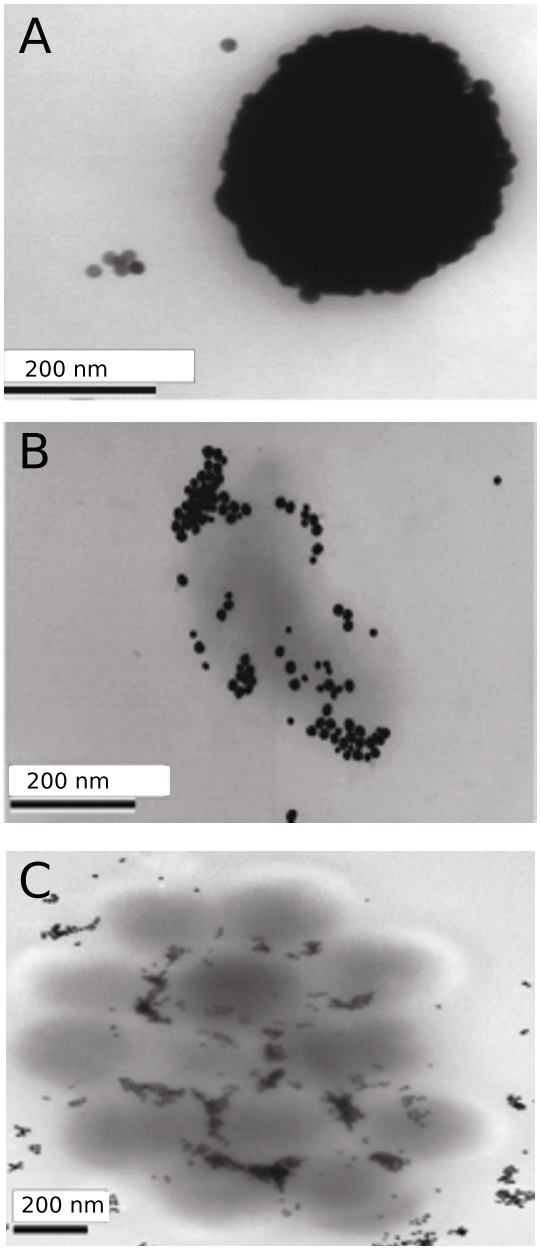

Figure 4 | Transmission electron microscopy of purified virions binding to gB-GNP. gB-GNPs conjugated to 100 ng antibody total (A) or 50 ng antibody total (B), (C) were added to purified virus particles and placed on a grid for electron microscopy. A single virion covered with gB-GNPs is shown (A), in comparison to a cluster of virions attaching to gB-GNPs (B), (C).

earlier[22]. Next, we performed the fluorescence analyses to determine the amount of dye-labeled antibody binding to nanoparticles. By dividing the total number of dye-labeled antibody by the total number of nanoparticles, we estimated that there were about 350–450 antibody per gold nanoparticle. We performed this experiment for nanoparticle of each shape and maintained the number of antibody molecule per particle at around 350–450. TEM images of antibody-conjugated gold nanoparticles of each shape are shown (extended data 5). To measure the size, zeta potential and polydispersity of antibody-conjugated gold nanoparticle, we used Malvern Zetasizer Nano instrument. The size of a single antibody conjugated spherical gold nanoparticle was about 44 ± 4 nm, while a single antibody conjugated popcorn gold nanoparticle was 47 ± 5 nm, and an antibody conjugated star-shape gold nanoparticle was 51 ± 4 nm. Zeta potential for an antibody conjugated spherical gold nanoparticle was determined to be −5.12 mV. Similarly for antibody-conjugated nano-popcorn, it was −3.28 mV and for antibody-conjugated nano-star it was −2.12 mV. Polydispersity Index (PDI) for each shape of antibody conjugated-nanoparticle was about 0.150.

Cells. Primary human foreskin-derived fibroblasts (HF) were cultured in Dulbecco's modified Eagle's medium (Invitrogen Corporation, Carlsbad, CA) containing 4.5 g/ml glucose, 10% fetal bovine serum (S1245OH; Atlanta Biologicals, Lawrenceville, GA), 1 mM sodium pyruvate, 2 mM L-glutamine, and 100 U/ml penicillin-streptomycin (Cellgro, Manassas, VA) at 37°C with 5% CO_2. Human microvascular endothelial cells (HMEC-1)[20] were cultured in MCDB31 medium (Bioworld, Dublin, OH) containing 4.5 g/ml glucose, 10% fetal bovine serum (S1245OH), 1 mM sodium pyruvate, 2 mM L-glutamine, and 100 U/ml penicillin-streptomycin at 37°C with 5% CO_2. The viability of cells was recorded by trypan blue exclusion on TC10 automated cell counter (BioRad, Hercules, CA) or by MTT assay as described earlier[22].

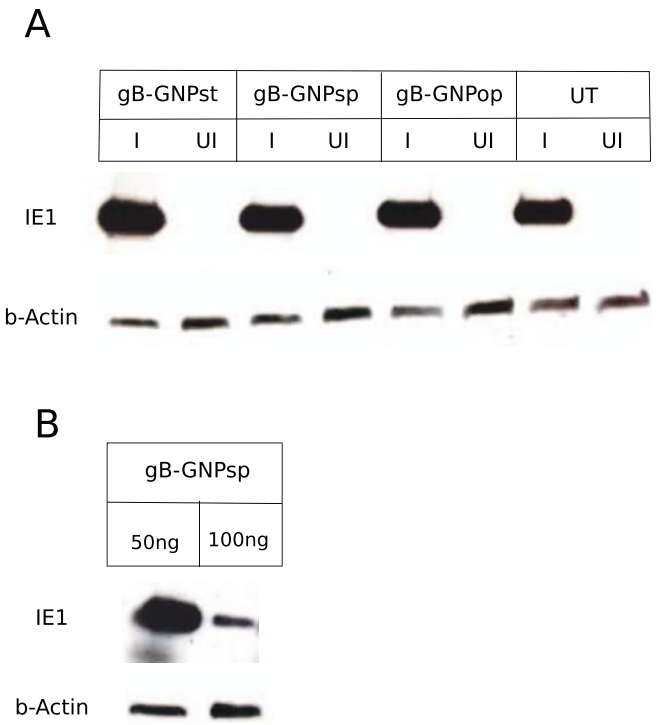

Figure 5 | gB-GNP interfere with CMV entry in fibroblasts, but only at higher concentrations. (A) HF were treated with 50 ng anti gB antibody conjugated to GNPst, GNPsp or GNPop or mock treated (UT) and then infected (I) with CMV (AD169) at an MOI of 3.0 or mock infected (UI). Cells were lysed at 6 hpi and probed for viral IE1 protein expression in an immunoblot. (B) HF were treated with 50 ng or 100 ng anti gB antibody conjugated to GNPsp and then infected with CMV (AD169) at an MOI of 3.0. Cells were lysed at 6 hpi and probed for viral IE1 protein expression in an immunoblot. b-actin was used as a loading control.

Virus. Human cytomegalovirus AD169, Towne, TB40/e and FIX strains have been reported earlier[19,25,26]. A version of AD169 virus where pp150 tegument protein has been fused with eGFP (BAD32 virus) was obtained from Moorman laboratory at University of North Carolina[18]. CMV virions were purified using established protocols for herpesviruses[27–29] with some modifications. Briefly, HF monolayers were infected with AD169 virus (MOI of 5), and harvested at 4 to 5 dpi. Medium was clarified of any cellular debris by low speed centrifugation (2000 g, 10 min) and virus particles were pelleted (~20000 g, 1 h). Virions were purified on a 15–50% sucrose gradient in phosphate buffer (40 mM mono-/dibasic phosphate, 150 mM NaCl, pH 7.4) using ultracentrifugation (SW 32Ti rotor, Beckman L-90 ultracentrifuge, 24000 rpm, 1 h). Virions were harvested by puncturing the sides of the centrifuge tube with a 23 G needle and were washed once in phosphate buffer before concentrating by centrifugation (SW-41 rotor, Beckman L-80 ultracentrifuge, 24000 rpm, 1 h). Identity and purity of harvested capsids was confirmed by electron microscopy.

Nanophotothermolysis. gB-GNPop (conjugated to 50 ng antibody total) were added to cells infected with AD169 strain of CMV at an MOI of 5, a range of MOI from 0.001 to 5.0 (B) or mock. After binding for 1 hour, gB-GNPop were washed off, so that only gB-GNPop that remain attached to infected cells are present on cells. Cells were exposed to 670 nm, 100 mW laser for 15 minutes and then subjected to a cell viability test (MTT).

Antibodies and immunoblot analyses. HF were harvested at 6 hpi for analysis of viral immediate early 1 (IE1) gene expression by immunoblotting (IB). Anti IE1 antibody (Virusys, Taneytown, MD) was used as the primary antibody and peroxidase-labeled horse anti-mouse IgG (Vector Laboratories, Burlingame, CA) was used as the secondary antibody for IBs. Blots were detected using ECL Western blotting detection reagents (GE Healthcare, Buckinghamshire, United Kingdom).

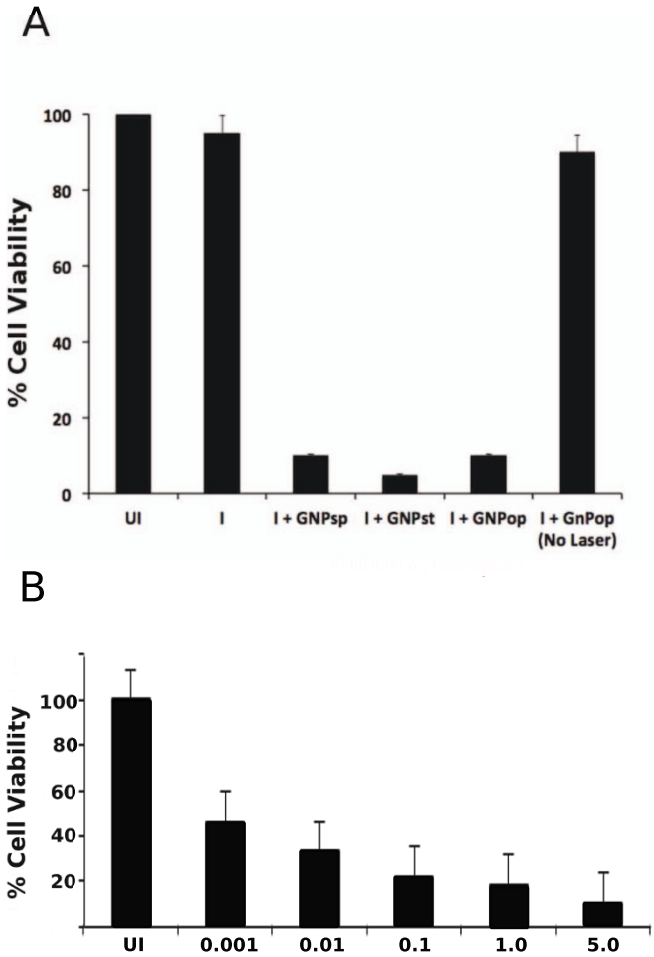

Figure 6 | Specific lysis of infected cells after gB-GNPop treatment and laser exposure. gB-GNPop (conjugated to 50 ng antibody total) were added to cells infected (I) with AD169 strain of CMV at an MOI of 5 (A), a range of MOI from 0.001 to 5.0 (B) or mock infected (UI). gB-GNPsp, gB-GNPst and gB-GNPop (A) or only gB-GNPop (B) were used for experiments. After binding for 1 hour, gB-GNP were washed off, so that only gB-GNP that remain attached to infected cells are present on cells. Cells were exposed to 670 nm, 100 mW laser for 15 minutes and then subjected to a cell viability test (MTT).

Microscopy. Samples were prepared using established protocols for immunofluorescence assay and fluorescence microscopy. Briefly, cells were grown on coverslip inserts in 24-well tissue culture dishes. At the end point, cells were fixed in either 3.7% formaldehyde for 10 min or 4% paraformaldehyde for 20 min and were incubated in 50 mM NH_4Cl in PBS for 10 min to reduce autofluorescence. This followed a wash, incubation in 0.5% Triton X-100 for 20 min to permeabilize the cells, and finally a wash and incubation with primary and secondary antibodies. Coverslips were retrieved from the wells and were mounted on glass slides with a drop of mounting medium (2.5% DABCO in Fluoromont G) and dried overnight before imaging. Images were acquired on a Zeiss Axio Imager A1 epifluorescent microscope. For electron microscopy, virions were first purified according to the established protocols[30] and then mixed with gB-GNP and incubated for one hour. Samples were placed on a TEM grid and imaging was performed on a high-resolution transmission electron microscope (JOEL 2100F).

1. Krause, P. R. *et al.* Priorities for CMV vaccine development. *Vaccine* **32**, 4–10 (2013).
2. Hakki, M. & Chou, S. The biology of cytomegalovirus drug resistance. *Curr. Opin. Infect. Dis.* **24**, 605–611 (2011).
3. Solanki, K. *et al.* Enzyme-based listericidal nanocomposites. *Sci Rep* **3**, 1584 (2013).
4. Fan, Z. *et al.* Multifunctional plasmonic shell-magnetic core nanoparticles for targeted diagnostics, isolation, and photothermal destruction of tumor cells. *ACS nano* **6**, 1065–1073 (2012).
5. Fan, Z. *et al.* Popcorn-shaped magnetic core-plasmonic shell multifunctional nanoparticles for the targeted magnetic separation and enrichment, label-free SERS imaging, and photothermal destruction of multidrug-resistant bacteria. *Chem. Eur. J.* **19**, 2839–2847 (2013).
6. Shen, S. *et al.* CMCTS stabilized Fe3O4 particles with extremely low toxicity as highly efficient near-infrared photothermal agents for in vivo tumor ablation. *Nanoscale* **5**, 8056–8066 (2013).
7. Singh, A. K. *et al.* Gold Nanorod Based Selective Identification of Escherichia coli Bacteria Using Two-Photon Rayleigh Scattering Spectroscopy. *ACS nano* **3**, 1906–1912 (2009).
8. Zharov, V. P., Mercer, K. E., Galitovskaya, E. N. & Smeltzer, M. S. Photothermal nanotherapeutics and nanodiagnostics for selective killing of bacteria targeted with gold nanoparticles. *Biophys. J.* **90**, 619–627 (2006).
9. Cabral, H., Nishiyama, N. & Kataoka, K. Supramolecular nanodevices: from design validation to theranostic nanomedicine. *Acc. Chem. Res.* **44**, 999–1008 (2011).
10. Dreaden, E. C., Mackey, M. A., Huang, X., Kang, B. & El-Sayed, M. A. Beating cancer in multiple ways using nanogold. *Chem Soc Rev* **40**, 3391–3404 (2011).
11. Ganta, S. & Amiji, M. Coadministration of Paclitaxel and curcumin in nanoemulsion formulations to overcome multidrug resistance in tumor cells. *Mol. Pharm.* **6**, 928–939 (2009).
12. Lane, D. Designer combination therapy for cancer. *Nat. Biotechnol.* **24**, 163–164 (2006).
13. Wang, S. *et al.* Multifunctional biodegradable polyacrylamide nanocarriers for cancer theranostics--a "see and treat" strategy. *ACS nano* **6**, 6843–6851 (2012).
14. Griffin, J. *et al.* Sequence-specific HCV RNA quantification using the size-dependent nonlinear optical properties of gold nanoparticles. *Small* **5**, 839–845 (2009).
15. Fan, Z., Senapati, D., Singh, A. K. & Ray, P. C. Theranostic magnetic core-plasmonic shell star shape nanoparticle for the isolation of targeted rare tumor cells from whole blood, fluorescence imaging, and photothermal destruction of cancer. *Mol. Pharm.* **10**, 857–866 (2013).
16. Beqa, L., Fan, Z., Singh, A. K., Senapati, D. & Ray, P. C. Gold nano-popcorn attached SWCNT hybrid nanomaterial for targeted diagnosis and photothermal therapy of human breast cancer cells. *ACS Appl Mater Interfaces* **3**, 3316–3324 (2011).
17. Khan, S. A., Singh, A. K., Senapati, D., Fan, Z. & Ray, P. C. Targeted highly sensitive detection of multi-drug resistant Salmonella DT104 using gold nanoparticles. *Chem. Commun. (Camb.)* **47**, 9444–9446 (2011).
18. Moorman, N. J., Sharon-Friling, R., Shenk, T. & Cristea, I. M. A targeted spatial-temporal proteomics approach implicates multiple cellular trafficking pathways in human cytomegalovirus virion maturation. *Mol. Cell Proteomics* **9**, 851–860 (2010).
19. Murphy, E. *et al.* Coding potential of laboratory and clinical strains of human cytomegalovirus. *Proc. Natl. Acad. Sci. U.S.A.* **100**, 14976–14981 (2003).
20. Ades, E. W. *et al.* HMEC-1: establishment of an immortalized human microvascular endothelial cell line. *J. Invest. Dermatol.* **99**, 683–690 (1992).
21. Mocarski, E. S., Jr., Shenk, T. & Pass, R. F. Cytomegaloviruses. p. 2701–2772. *In* Knipe, D. M. & Howley, P. M. (ed.), *Fields Virology. 5th Edition. Lippincott Williams & Wilkins, Philadelphia*. (2006).
22. Lu, W. *et al.* Gold nano-popcorn-based targeted diagnosis, nanotherapy treatment, and in situ monitoring of photothermal therapy response of prostate cancer cells using surface-enhanced Raman spectroscopy. *J. Am. Chem. Soc.* **132**, 18103–18114 (2010).
23. Senapati, D., Singh, A. K., Khan, S. A., Senapati, T. & Ray, P. C. Probing real time gold nanostar formation process using two-photon scattering spectroscopy. *Chem Phys Lett* **504**, 46–51 (2011).
24. Ray, P. C., Khan, S. A., Singh, A. K., Senapati, D. & Fan, Z. Nanomaterials for targeted detection and photothermal killing of bacteria. *Chem Soc Rev* **41**, 3193–3209 (2012).
25. Yu, D., Silva, M. C. & Shenk, T. Functional map of human cytomegalovirus AD169 defined by global mutational analysis. *Proc. Natl. Acad. Sci. U.S.A.* **100**, 12396–12401 (2003).
26. Dunn, W. *et al.* Functional profiling of a human cytomegalovirus genome. *Proc. Natl. Acad. Sci. U.S.A.* **100**, 14223–14228 (2003).
27. Gibson, W. Protein counterparts of human and simian cytomegaloviruses. *Virology* **128**, 391–406 (1983).
28. Irmiere, A. & Gibson, W. Isolation of human cytomegalovirus intranuclear capsids, characterization of their protein constituents, and demonstration that the B-capsid assembly protein is also abundant in noninfectious enveloped particles. *J. Virol.* **56**, 277–283 (1985).
29. Thomsen, D. R., Newcomb, W. W., Brown, J. C. & Homa, F. L. Assembly of the herpes simplex virus capsid: requirement for the carboxyl-terminal twenty-five amino acids of the proteins encoded by the UL26 and UL26.5 genes. *J. Virol.* **69**, 3690–3703 (1995).
30. Tandon, R. & Mocarski, E. S. Cytomegalovirus pUL96 is critical for the stability of pp150-associated nucleocapsids. *J. Virol.* **85**, 7129–7141 (2011).

Acknowledgments

We thank Andrew Yurochko, Edward S. Mocarski and Vaibhav Tiwari for helpful discussions during the preparation of this manuscript. We thank Felicia Goodrum for the FIX-BAC, Nathaniel Moorman for the BAD32GFP virus and Prashant Desai for the

K26GFP virus. This work was supported by Intramural Research Support Award from University of Mississippi Medical Center to Ritesh Tandon and NSF-PREM grant (# DMR-1205194) awards to Paresh C. Ray.

Author contributions

P.C.R. conceived and designed the nanoparticle synthesis and their conjugation to antibody. R.T. conceived and designed the CMV experiments. Z.F. synthesized and conjugated the nanoparticles and performed experiments involving laser as well as electron microscopy. R.T., B.M.D. and M.A.A. performed the CMV experiments. R.T. and P.C.R. analyzed the data and prepared the figures. All authors edited the paper.

Additional information

Supplementary information accompanies this paper at http://www.nature.com/scientificreports

Competing financial interests: The authors declare no competing financial interests.

How to cite this article: DeRussy, B.M., Aylward, M.A., Fan, Z., Ray, P.C. & Tandon, R. Inhibition of cytomegalovirus infection and photothermolysis of infected cells using bioconjugated gold nanoparticles. *Sci. Rep.* **4**, 5550; DOI:10.1038/srep05550 (2014).